AD-A118 382   ARMY ARMAMENT RESEARCH AND DEVELOPMENT COMMAND WATER--ETC F/G 20/11

A PHOTOELASTIC STUDY OF LOAD DISTRIBUTIONS AND STRESSES IN MULT--ETC(U)

MAY 82   Y F CHENG

UNCLASSIFIED   ARLCB-TR-82013   SBI-AD-E440 155   NL

1 of 1

AD A118382

END

DATE FILMED

09-82

DTIC

TECHNICAL REPORT ARLCB-TR-82013

A PHOTOELASTIC STUDY OF LOAD DISTRIBUTIONS AND STRESSES IN MULTI-GROOVE CONNECTIONS OF THE SAME MATERIAL UNDER TENSION

Y. F. Cheng

May 1982

US ARMY ARMAMENT RESEARCH AND DEVELOPMENT COMMAND
LARGE CALIBER WEAPON SYSTEMS LABORATORY
BENÉT WEAPONS LABORATORY
WATERVLIET, N. Y. 12189

AMCMS No. 61110191A0011

DA Project No. 1L161101A91A

PRON No. 1A2231491A1A

APPROVED FOR PUBLIC RELEASE; DISTRIBUTION UNLIMITED

DISCLAIMER

The findings in this report are not to be construed as an official Department of the Army position unless so designated by other authorized documents.

The use of trade name(s) and/or manufacture(s) does not constitute an official indorsement or approval.

DISPOSITION

Destroy this report when it is no longer needed. Do not return it to the originator.

SECURITY CLASSIFICATION OF THIS PAGE (When Data Entered)

REPORT DOCUMENTATION PAGE

READ INSTRUCTIONS BEFORE COMPLETING FORM

1. REPORT NUMBER ARLCB-TR-82013	2. GOVT ACCESSION NO. AD-A118 382	3. RECIPIENT'S CATALOG NUMBER
4. TITLE (and Subtitle) A PHOTOELASTIC STUDY OF LOAD DISTRIBUTIONS AND STRESSES IN MULTI-GROOVE CONNECTIONS OF THE SAME MATERIAL UNDER TENSION		5. TYPE OF REPORT & PERIOD COVERED 6. PERFORMING ORG. REPORT NUMBER
7. AUTHOR(s) Y. F. Cheng		8. CONTRACT OR GRANT NUMBER(s)
9. PERFORMING ORGANIZATION NAME AND ADDRESS US Army Armament Research & Development Command Benet Weapons Laboratory, DRDAR-LCB-TL Watervliet, NY 12189		10. PROGRAM ELEMENT, PROJECT, TASK AREA & WORK UNIT NUMBERS AMCMS No. 61110191A0011 DA Project No. 1L161101A9A PRON No. 1A2231491A1A
11. CONTROLLING OFFICE NAME AND ADDRESS US Army Armament Research & Development Command Large Caliber Weapon Systems Laboratory Dover, NJ 07801		12. REPORT DATE May 1982 13. NUMBER OF PAGES 23
14. MONITORING AGENCY NAME & ADDRESS(if different from Controlling Office)		15. SECURITY CLASS. (of this report) UNCLASSIFIED 15a. DECLASSIFICATION/DOWNGRADING SCHEDULE

16. DISTRIBUTION STATEMENT (of this Report)

Approved for public release; distribution unlimited.

17. DISTRIBUTION STATEMENT (of the abstract entered in Block 20, if different from Report)

18. SUPPLEMENTARY NOTES

19. KEY WORDS (Continue on reverse side if necessary and identify by block number)

Groove Connections
Photoelasticity
Maximum Fillet Stresses
Load Distributions
Stress Concentrations
Stress Distributions
Critical Regions

20. ABSTRACT (Continue on reverse side if necessary and identify by block number)

This report is a continuation of Technical Report ARLCB-TR-81008 and describes a three-dimensional photoelastic study on load distributions and stresses in multi-groove connections of the same material under tension. Two groove profiles were investigated, namely, the British Standard Buttress (BSB), and the new profile. It was found that in both profiles the maximum fillet stress $(\sigma_f)_{max}$ does not occur at the groove root. Therefore, the narrowest transverse

(CONT'D ON REVERSE)

DD FORM 1 JAN 73 1473 EDITION OF 1 NOV 65 IS OBSOLETE

UNCLASSIFIED

SECURITY CLASSIFICATION OF THIS PAGE (When Data Entered)

20. ABSTRACT (CONT'D)

section is not the critical section. The critical stress, i.e., $(\sigma_f)_{max}$, in the new profile is higher than that in the BSB profile. Moreover, $(\sigma_f)_{max}$ in the first groove is higher than that in subsequent grooves. Hence, the first groove is the critical region.

In an ideal multi-groove (> 7) connection, the first two lugs could take approximately 50 and 60 percent of the load in the BSB and new profile, respectively. However, the ideal contact could not be expected due to machining tolerances. The worst possible case would occur when only one groove is in contact and the situation is reduced to a single-groove connection.

Further work on the effect of different materials is in progress.

TABLE OF CONTENTS

TABLES

LIST OF ILLUSTRATIONS

ACKNOWLEDGEMENT

Charles Cobb's participation in the experimental phase of this investigation is hereby acknowledged.

INTRODUCTION

This report is a continuation of Technical Report ARLCB-TR-81008[1] which dealt with the maximum fillet stress and the critical region in single-groove connections of the same material under axial tension. This investigation arose out of a study of critical stresses at the core of penetrators. In a penetrator, the core and the sabot are in contact through a series of lugs and grooves. The core of a penetrator with British Standard Buttress (BSB) grooves failed transversely near the fillet of the rearmost groove during a test. The failure was brittle indicating the presence of a high tensile stress. A study was made in FY80 to determine the critical stresses in single-groove connections of the same material under axial tension. Two groove profiles were included, namely, the BSB profile, Figure 1, and a new profile, Figure 2. The results showed that in the former case, the maximum fillet stress $(\sigma_f)_{max}$ had a value of 61 psi at a point approximately 21 degrees from the narrowest section toward the loaded face, Figure 3(a). In the latter case $(\sigma_f)_{max}$ had a value of 98 psi at a point approximately 43 degrees from the narrowest section, Figure 3(b). Moreover, $(\sigma_f)_{max}$ was the critical stress and the critical region was the region where $(\sigma_f)_{max}$ was located.

The objectives of the present work were to determine the maximum fillet stress, the critical region, and the load distribution among grooves in multi-groove connections of the same material under axial tension. The same

[1]Cheng, Y. F., "A Photoelastic Study of Stresses in Single-Groove Connections of the Same Material," Technical Report ARLCB-TR-81008, USA ARRADCOM, Benet Weapons Laboratory, Watervliet, NY, February 1981.

two groove profiles as reported previously were studied. All data were obtained photoelastically by means of the three-dimensional shear-difference method in combination with stress-freezing-and-slicing techniques.

In a penetrator, the core and the sabot are usually made of different materials. However, the present investigation was limited to the same material. Further work on the effect of different materials is in progress. The results will be reported at a later date.

EXPERIMENTAL PROCEDURE

Two models of seven-groove connections were constructed of photoelastic model material PLM4B, supplied by Measurement Group, Raleigh, NC. Figure 4 shows a photograph of the first model with BSB grooves. The sabot consisted of two semi-cylinders. They were cemented together after assembly with dowel pins made of the same material for alignment.

The model was loaded by means of dead weights in a stress-freezing furnace. The loaded model and calibration disks were slowly heated in the furnace to the critical temperature of 250°F, held constant for eight hours, and then gradually cooled to room temperature at which time the loads were removed. The rate of heating was 10°F/hour and of cooling 1°F/hour with a duration of the cycle about eight to nine days. The loads were 60 pounds in both models including body weight of the sabot.

One meridian slice of 0.1 inch thick was removed from the core of each model after stress freezing for photoelastic observations. The plane of the slice was 90 degrees from the cement joint.

The equipment employed in the investigation, the precision of measurement, and a brief review of the shear-difference method can be found in the previous report ARLCB-TR-81008, and will not be repeated here.

EXPERIMENTAL RESULTS

Radial Distributions of Stress σ_r, σ_z, and τ_{rz}

By means of shear-difference method, radial distributions of stresses σ_r, σ_z, and τ_{rz} were determined on seven transverse sections passing through groove roots in both models. Figures 5(a) and 5(b) show a typical distribution of these stresses in each model, respectively. As would be expected, in every section the maximum of σ_z occurred on the root of the groove indicating the notch effect. Due to the interest of preserving the slices, sub-slices were not prepared and values of σ_θ were not determined.

Section Load and Lug Load

Axial load P_i was found for each section by integrating $(\sigma_z)_i$ over the section. Thus $P_i = 2\pi\int(\sigma_z)_i rdr$ where subscript i denotes quantities relating to the i^{th} section. Neglecting body force, the individual lug load is equal to the difference in loads between neighboring sections. This is shown in Figures 6(a) and 6(b).

Maximum Fillet Stress $(\sigma_f)_{max}$ and Stress Concentration Factor K

Maximum fillet stress $(\sigma_f)_{max}$ was determined for the first three grooves in both models. They were always located at some angular distance away from the narrowest transverse section toward the loaded face. Stress concentration factor K was calculated by defining $K = (\sigma_f)_{max}/(P/A)$ where P is the axial load and A the cross-sectional area. Table I shows the values of $(\sigma_f)_{max}$ and

K. It can be seen that $(\sigma_f)_{max}$ is influenced by both the section load and the lug load. For example, the value of $(\sigma_f)_{max}$ in the first groove of new profile multi-connection is about 76 percent of that in the single-connection, while very little difference in section loads between them exists (61.2 versus 58.8). The difference in $(\sigma_f)_{max}$ is due mostly to lug load. In the BSB profile, the second lug had a load almost twice that of the first lug. The fact that $(\sigma_f)_{max}$ of the second groove is less than that of the first groove demonstrates the influence of the section load.

TABLE I. VALUES OF SECTION, LUG LOAD, $(\sigma_f)_{max}$, K, AND $(\sigma_z)_{max}$

Section No.	Section Load Pounds	Lug Load Pounds	$(\sigma_f)_{max}$ psi	K	$(\sigma_z)_{max}$ psi
BSB Profile, Multi-Connection					
1	59.9	10.5	50	3.7	48
2	49.4	19.4	48	3.6	33
3	30.0	3.3	29	2.1	17
BSB Profile, Single Connection					
	59.1	59.1	61	4.6	54
New Profile, Multi-Connection					
1	61.2	21.1	76	5.3	37
2	40.1	15.6	57	4.0	20
3	24.5	7.8	50	3.5	11
New Profile, Single Connection					
	58.8	58.8	98	7.1	42

Distribution of Shear Stress τ_{rz}

Distribution of shear stress τ_{rz} was determined on the surface of cylindrical sections passing through groove roots. Figures 7(a) and 7(b) show typical distributions in each model. It can be seen that the maximum value of $|\tau_{rz}|$ in the new profile is lower than that in the BSB profile.

DISCUSSION

Critical Regions

In both models the maximum fillet stress $(\sigma_f)_{max}$ was found at a point some angular distance away from the narrowest transverse section toward the loaded face. Table I also shows a comparison between $(\sigma_f)_{max}$ and $(\sigma_z)_{max}$ for the first three grooves in each model. It can be seen that in each groove $(\sigma_f)_{max}$ is always greater than $(\sigma_z)_{max}$. Hence $(\sigma_f)_{max}$ is the critical stress. In the new profile, $(\sigma_f)_{max}$ is a maximum at the first groove and decreases monotonically in subsequent lugs as the section load and lug load are simultaneously reduced. While the section load always decreases monotonically, the lug load is influenced by the contact condition. It can be seen that, in the BSB profile, the second lug had a load almost twice that of the first lug. (This is a particular case. It does not imply that the BSB profile always has this type of lug load distribution.) However, $(\sigma_f)_{max}$ in the first groove is still slightly higher than that in the second groove. In a normal case, the first section is the critical section; $(\sigma_f)_{max}$ in the first groove is the critical stress. Failure will occur when this stress reaches the ultimate value when loads are increased. The area where $(\sigma_f)_{max}$ is located is the critical region.

Checks

Two independent checks were made.

1. The condition of static equilibrium dictates that the load sustained by the first section is equal to the applied load. This condition is met by the fact that the applied load was 60 pounds in both models and the first section load was 59.9 and 61.2 pounds in the model with BSB and new profile, respectively, Figures 6(a) and 6(b).

2. The lug load can be found alternately by integrating τ_{rz} over the cylindrical section between lugs; i.e., $2\pi r\int\tau_{rz}dz$. Table II shows the results for the first three lugs as well as a comparison with those obtained by taking the difference between neighboring section loads. A good agreement exists.

TABLE II. LUG LOADS DETERMINED BY TWO METHODS

Section No.	Lug Load (pounds) Method 1	Lug Load (pounds) Method 2
BSB Profile		
1	10.5	10.0
2	19.4	20.1
3	3.3	3.4
New Profile		
1	21.1	20.6
2	15.6	14.8
3	7.8	7.3

Method 1: Taking difference between neighboring section loads.

Method 2: Integrating τ_{rz}.

Load Distributions

Experimental results show that in seven-groove connections the first two lugs took 50 and 60 percent of the load in the BSB and new profile, respectively, Figures 6(a) and 6(b). It is conservative in applying this figure to connections of more than seven grooves.

CONCLUSIONS

Stresses and load distributions in multi-groove connections of the same material under axial tension were studied photoelastically by means of the three-dimensional shear-difference method in combination with stress-freezing-and-slicing techniques. Two groove profiles were studied, namely, the British Standard Buttress and the new profile. The results show that, in both profiles, maximum fillet stress $(\sigma_f)_{max}$ does not occur at the groove root. Therefore, the narrowest transverse section is not the critical section. Also, the critical stress, i.e., $(\sigma_f)_{max}$, in the new profile is higher than that in the BSB profile. These findings are consistent with previous results obtained from single-groove connections (ARLCB-TR-81008). Moreover, $(\sigma_f)_{max}$ in the first groove is higher than that in subsequent grooves. Hence, the first groove is the critical region.

In a multi-groove connection under ideal contact, the load in the first lug is a maximum and decreases monotonically in subsequent lugs. Experimental results show that ideal contact does not always exist. For example, Figure 6(a) suggests that in the first model (BSB profile) the second lug made the initial contact, and with a possible contact sequence of 2-5-4-1-7-3-6. Realizing that ideal contact could not be expected due to machining

tolerances, the worst possible case would occur when only one lug is in contact and the situation is reduced to a single-groove connection with much higher value of $(\sigma_f)_{max}$, Table I. In an ideal multi-groove connection, the first two lugs could take approximately 50 and 60 percent of load in the BSB and new profile, respectively.

REFERENCES

1. Cheng, Y. F., "A Photoelastic Study of Stresses in Single-Groove Connections of the Same Material," Technical Report ARLCB-TR-81008, USA ARRADCOM, Benet Weapons Laboratory, Watervliet, NY, February 1981.

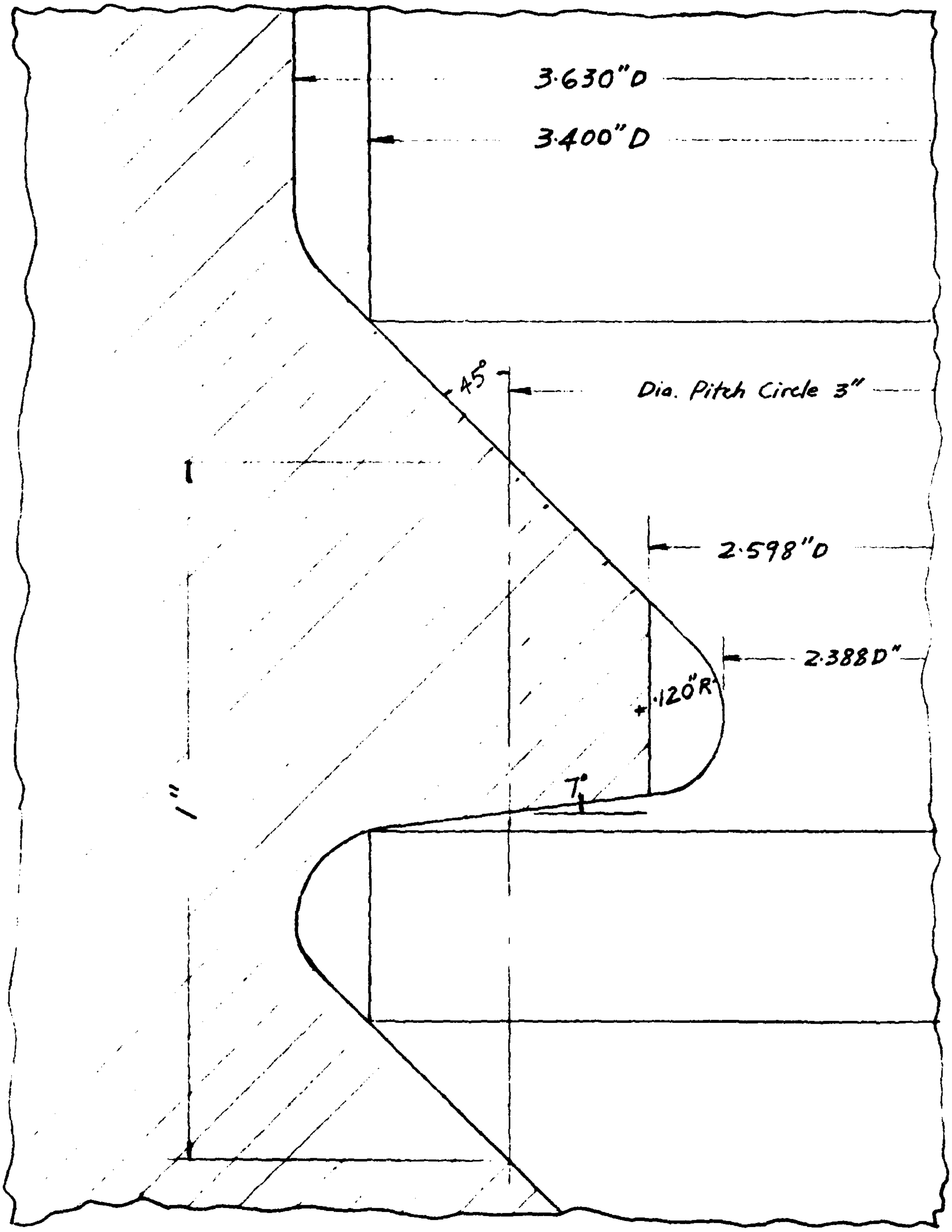

Figure 1. British standard buttress profile

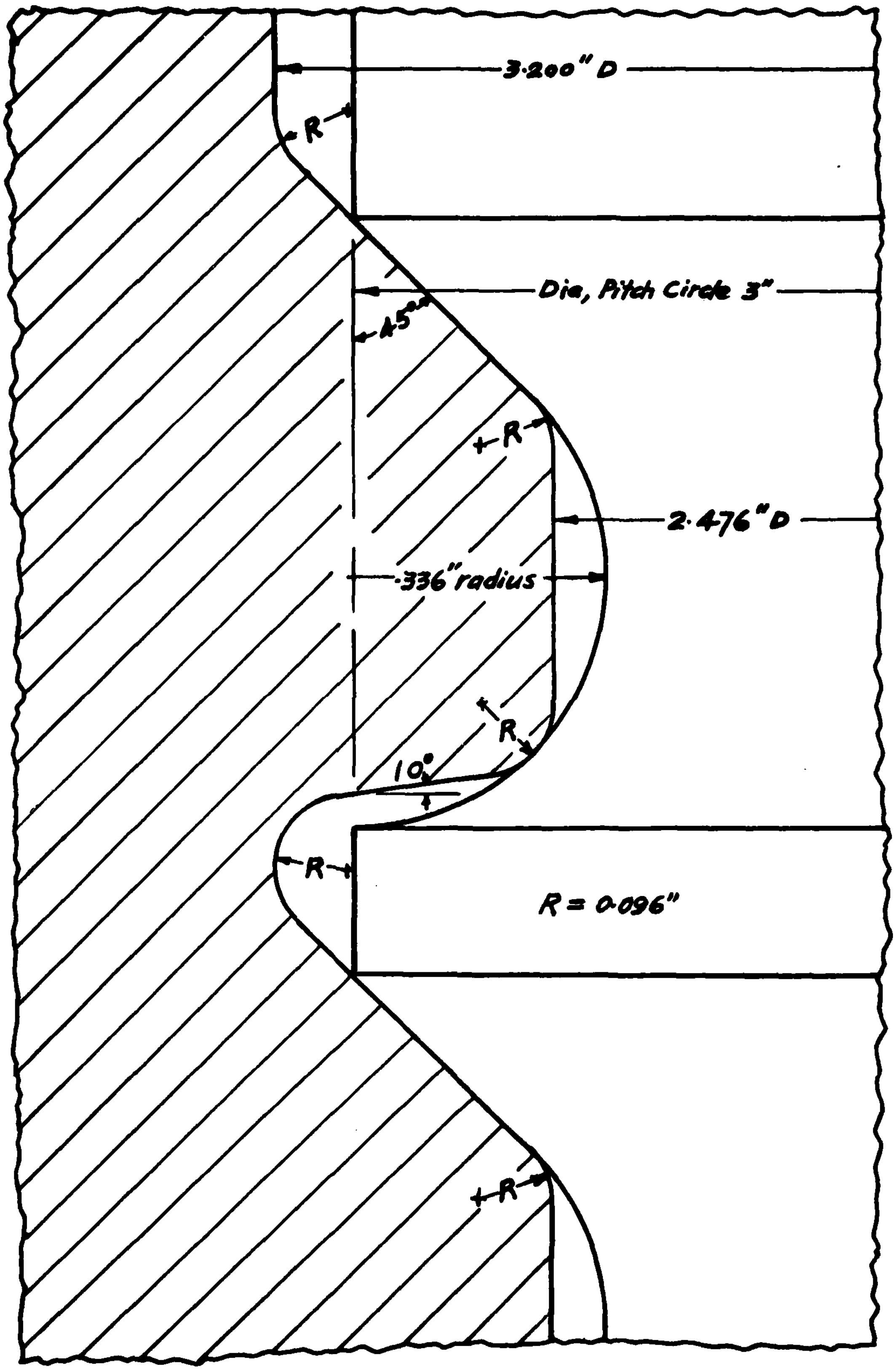

Figure 2. New profile

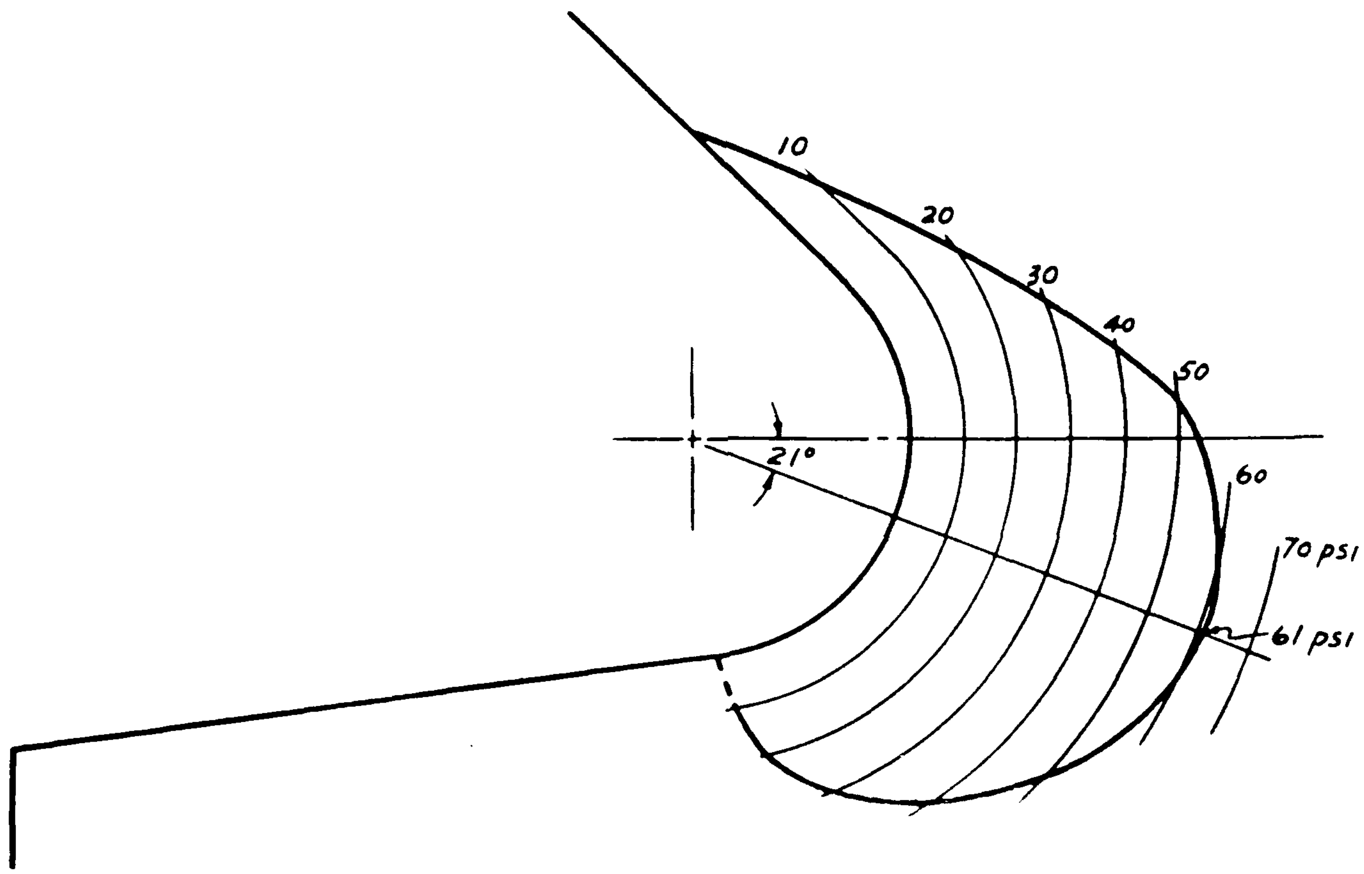

Figure 3. Distribution of fillet boundary stress in single-groove model, (a) BSB profile

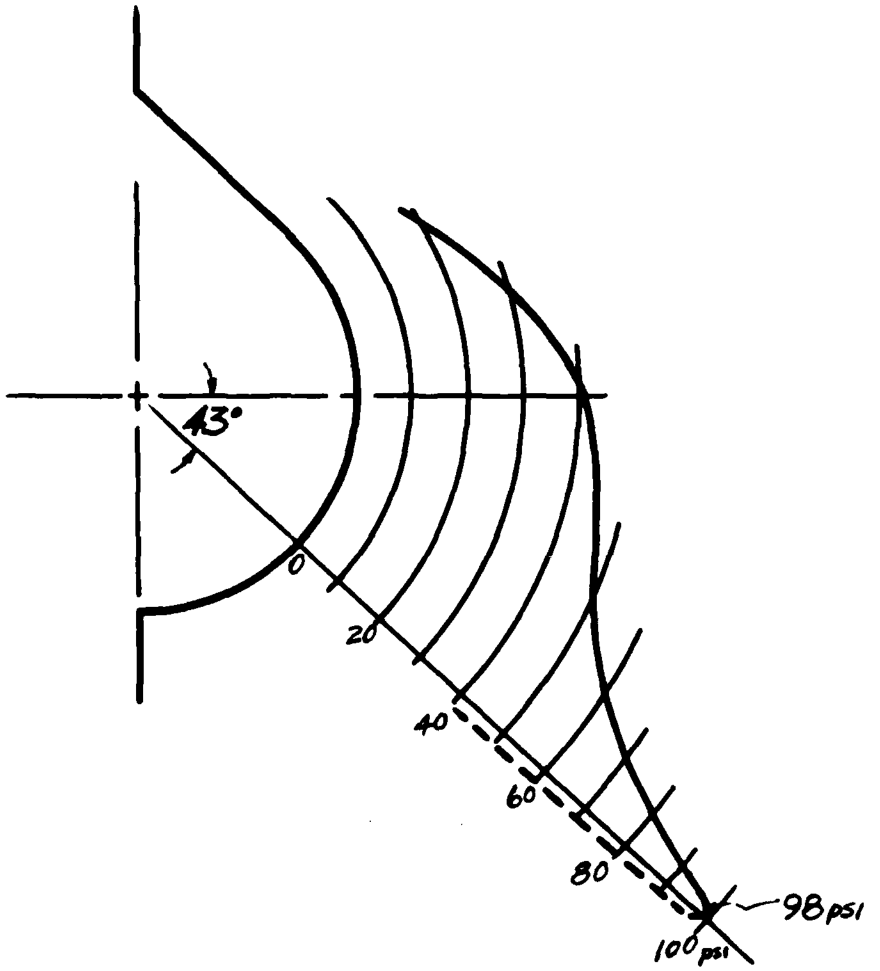

Figure 3. Distribution of fillet boundary stress in single-groove model.
(b) New profile

Figure 4. Photograph of the first multi-groove model, BSB profile

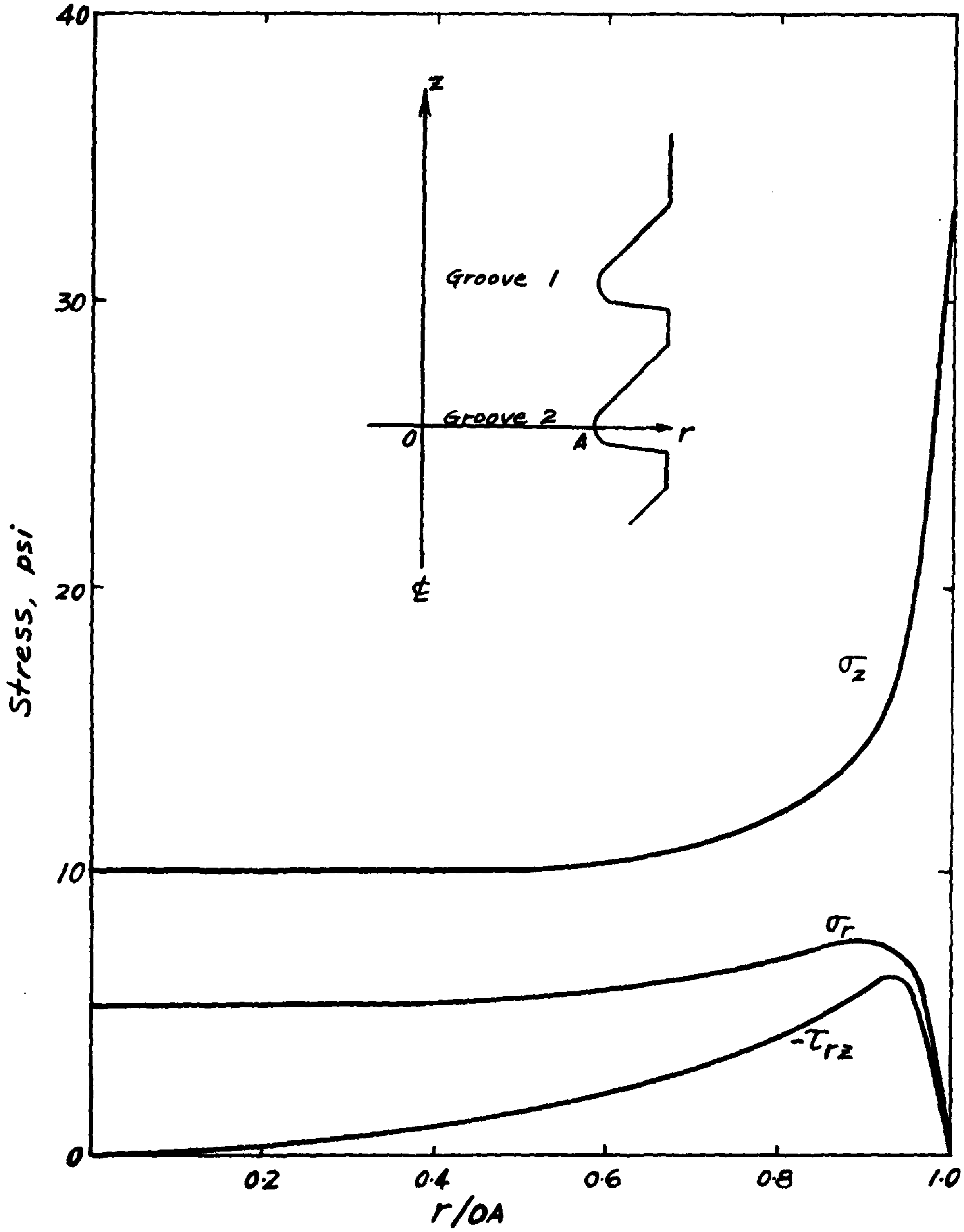

Figure 5. Typical distribution of σ_r, σ_z, and τ_{rz} on the transverse section of a multi-groove model, (a) BSB profile

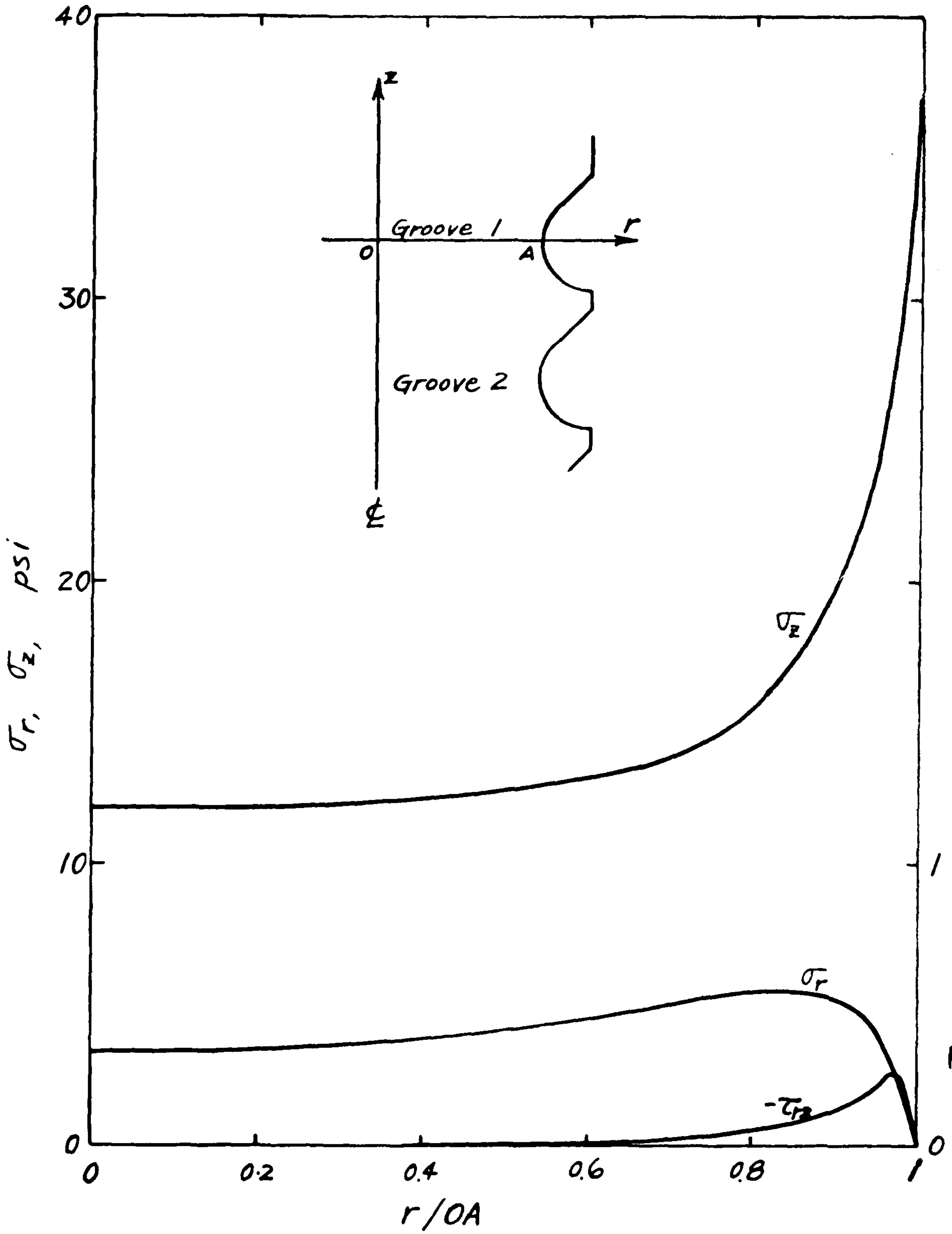

Figure 5. Typical distribution of σ_r, σ_z, and τ_{rz} on the transverse section of a multi-groove model, (b) New profile

Groove No.	Section Load pound	%	Lug Load pound
1	59.9	100	10.5
2	49.4	82.5	19.4
3	30.0	50.1	3.3
4	26.7	44.5	8.7
5	18.0	30.1	11.2
6	6.6	11.0	1.8
7	4.8	8.0	4.8

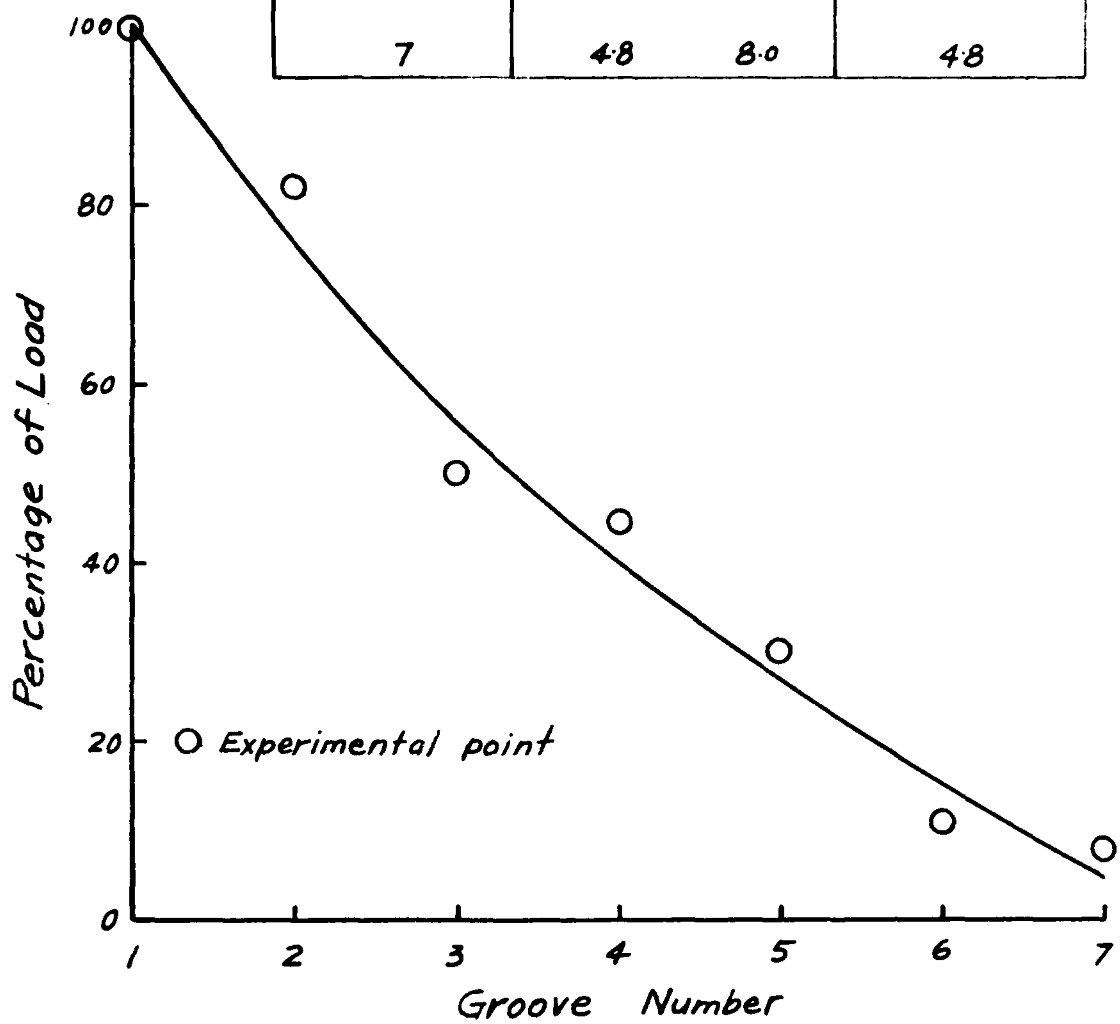

Figure 6. Load distributions

(a) BSB profile

Groove No	Section Load pound	Section Load %	Lug Load pound
1	61.2	100	21.1
2	40.1	65.6	15.6
3	24.5	40.1	7.8
4	16.7	27.3	4.4
5	12.3	20.1	5.8
6	6.5	10.6	1.5
7	5.0	8.2	5.0

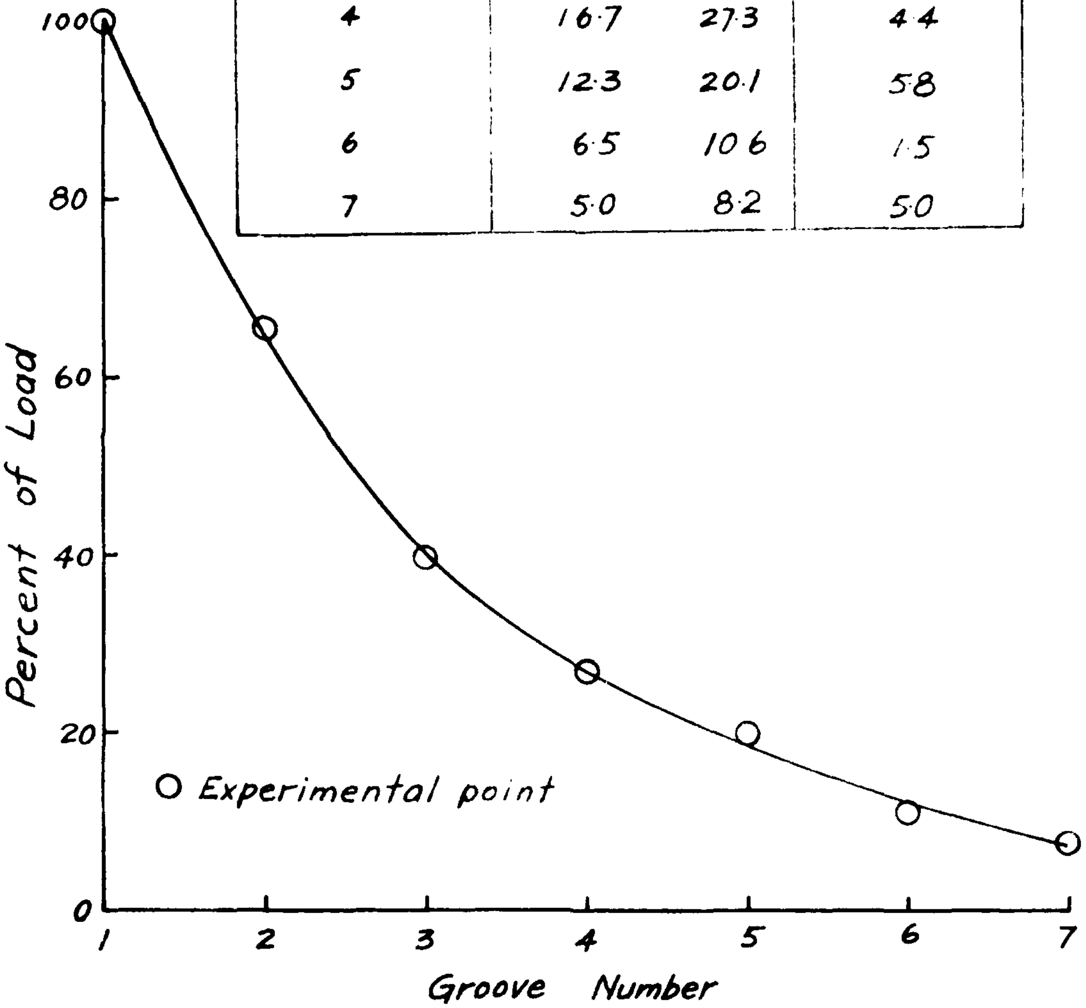

Figure 6. Load distributions
(b) New profile

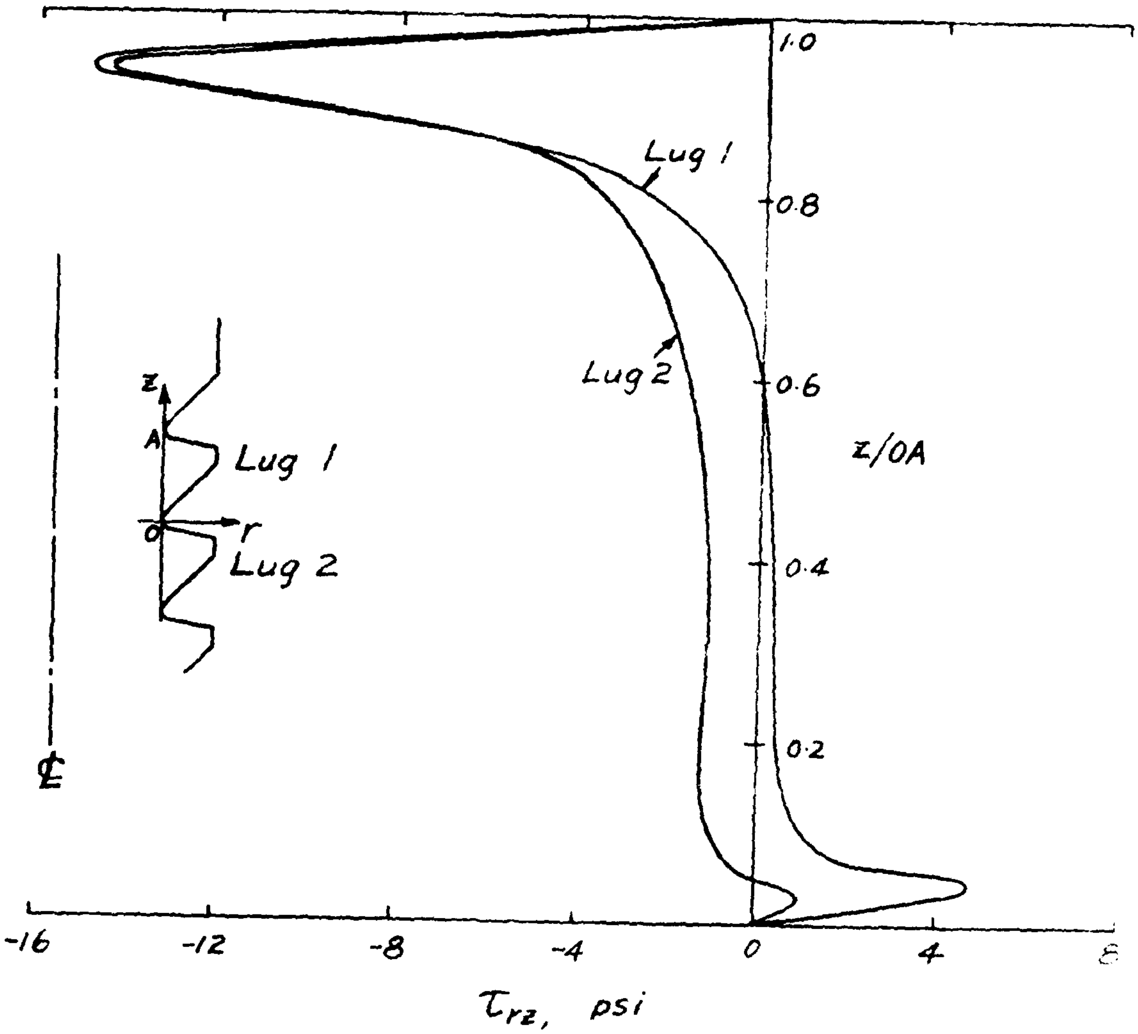

Figure 7. Typical distribution of τ_{rz} on surface of cylindrical section
(a) BSB profile

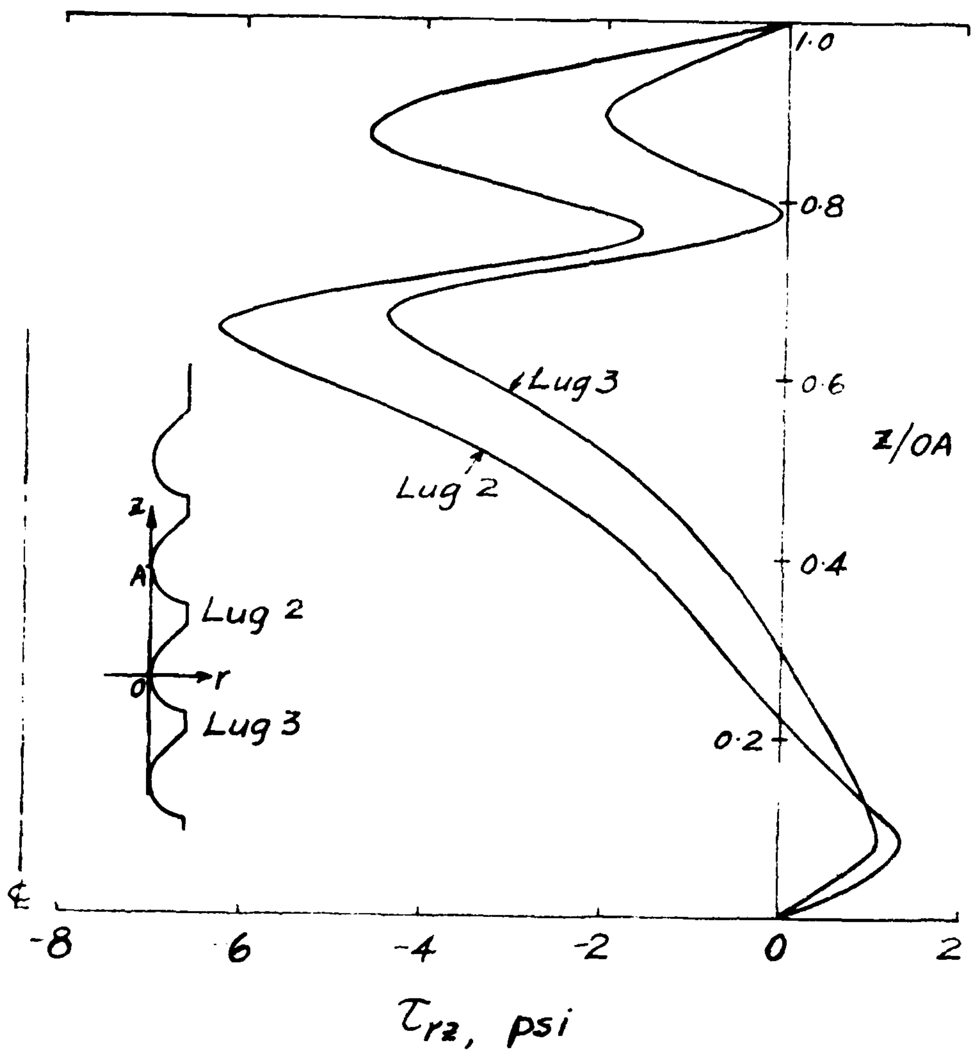

Figure 7. Typical distribution of τ_{rz} on surface of cylindrical section
(b) New profile

TECHNICAL REPORT INTERNAL DISTRIBUTION LIST

	NO. OF COPIES
COMMANDER	1
CHIEF, DEVELOPMENT ENGINEERING BRANCH	1
ATTN: DRDAR-LCB-DA	1
-DM	1
-DP	1
-DR	1
-DS (SYSTEMS)	1
-DS (ICAS GROUP)	1
-DC	1
CHIEF, ENGINEERING SUPPORT BRANCH	1
ATTN: DRDAR-LCB-SE	1
-SA	1
CHIEF, RESEARCH BRANCH	2
ATTN: DRDAR-LCB-RA	1
-RC	1
-RM	1
-RP	1
TECHNICAL LIBRARY	5
ATTN: DRDAR-LCB-TL	
TECHNICAL PUBLICATIONS & EDITING UNIT	2
ATTN: DRDAR-LCB-TL	
DIRECTOR, OPERATIONS DIRECTORATE	1
DIRECTOR, PROCUREMENT DIRECTORATE	1
DIRECTOR, PRODUCT ASSURANCE DIRECTORATE	1

NOTE: PLEASE NOTIFY DIRECTOR, BENET WEAPONS LABORATORY, ATTN: DRDAR-LCB-TL, OF ANY REQUIRED CHANGES.

TECHNICAL REPORT EXTERNAL DISTRIBUTION LIST

	NO. OF COPIES
ASST SEC OF THE ARMY	
RESEARCH & DEVELOPMENT	
ATTN: DEP FOR SCI & TECH	1
THE PENTAGON	
WASHINGTON, D.C. 20315	
COMMANDER	
US ARMY MAT DEV & READ. COMD	
ATTN: DRCDE	1
5001 EISENHOWER AVE	
ALEXANDRIA, VA 22333	
COMMANDER	
US ARMY ARRADCOM	
ATTN: DRDAR-LC	1
-LCA (PLASTICS TECH EVAL CEN)	1
-LCE	1
-LCM	1
-LCS	1
-LCW	1
-TSS (STINFO)	2
DOVER, NJ 07801	
COMMANDER	
US ARMY ARRCOM	
ATTN: DRSAR-LEP-L	1
ROCK ISLAND ARSENAL	
ROCK ISLAND, IL 61299	
DIRECTOR	
US ARMY BALLISTIC RESEARCH LABORATORY	
ATTN: DRDAR-TSB-S (STINFO)	1
ABERDEEN PROVING GROUND, MD 21005	
COMMANDER	
US ARMY ELECTRONICS COMD	
ATTN: TECH LIB	1
FT MONMOUTH, NJ 07703	
COMMANDER	
US ARMY MOBILITY EQUIP R&D COMD	
ATTN: TECH LIB	1
FT BELVOIR, VA 22060	

	NO. OF COPIES
COMMANDER	
US ARMY TANK-AUTMV R&D COMD	
ATTN: TECH LIB - DRDTA-UL	1
MAT LAB - DRDTA-RK	1
WARREN, MICHIGAN 48090	
COMMANDER	
US MILITARY ACADEMY	
ATTN: CHMN, MECH ENGR DEPT	1
WEST POINT, NY 10996	
US ARMY MISSILE COMD	
REDSTONE SCIENTIFIC INFO CEN	
ATTN: DOCUMENTS SECT, BLDG 4484	2
REDSTONE ARSENAL, AL 35898	
COMMANDER	
REDSTONE ARSENAL	
ATTN: DRSMI-RRS	1
-RSM	1
ALABAMA 35809	
COMMANDER	
ROCK ISLAND ARSENAL	
ATTN: SARRI-ENM (MAT SCI DIV)	1
ROCK ISLAND, IL 61299	
COMMANDER	
HQ, US ARMY AVN SCH	
ATTN: OFC OF THE LIBRARIAN	1
FT RUCKER, ALABAMA 36362	
COMMANDER	
US ARMY FGN SCIENCE & TECH CEN	
ATTN: DRXST-SD	1
220 7TH STREET, N.E.	
CHARLOTTESVILLE, VA 22901	
COMMANDER	
US ARMY MATERIALS & MECHANICS RESEARCH CENTER	
ATTN: TECH LIB - DRXMR-PL	2
WATERTOWN, MASS 02172	

NOTE: PLEASE NOTIFY COMMANDER, ARRADCOM, ATTN: BENET WEAPONS LABORATORY, DRDAR-LCB-TL, WATERVLIET ARSENAL, WATERVLIET, N.Y. 12189, OF ANY REQUIRED CHANGES.

TECHNICAL REPORT EXTERNAL DISTRIBUTION LIST (CONT.)

	NO. OF COPIES
COMMANDER US ARMY RESEARCH OFFICE P.O. BOX 12211 RESEARCH TRIANGLE PARK, NC 27709	1
COMMANDER US ARMY HARRY DIAMOND LAB ATTN: TECH LIB 2800 POWDER MILL ROAD ADELPHIA, MD 20783	1
DIRECTOR US ARMY INDUSTRIAL BASE ENG ACT ATTN: DRXPE-MT ROCK ISLAND, IL 61299	1
CHIEF, MATERIALS BRANCH US ARMY R&S GROUP, EUR BOX 65, FPO N.Y. 09510	1
COMMANDER NAVAL SURFACE WEAPONS CEN ATTN: CHIEF, MAT SCIENCE DIV DAHLGREN, VA 22448	1
DIRECTOR US NAVAL RESEARCH LAB ATTN: DIR, MECH DIV CODE 26-27 (DOC LIB) WASHINGTON, D.C. 20375	1 1
NASA SCIENTIFIC & TECH INFO FAC P.O. BOX 8757, ATTN: ACQ BR BALTIMORE/WASHINGTON INTL AIRPORT MARYLAND 21240	1

	NO. OF COPIES
COMMANDER DEFENSE TECHNICAL INFO CENTER ATTN: DTIA-TCA CAMERON STATION ALEXANDRIA, VA 22314	12 (2-LTD)
METALS & CERAMICS INFO CEN BATTELLE COLUMBUS LAB 505 KING AVE COLUMBUS, OHIO 43201	1
MECHANICAL PROPERTIES DATA CTR BATTELLE COLUMBUS LAB 505 KING AVE COLUMBUS, OHIO 43201	1
MATERIEL SYSTEMS ANALYSIS ACTV ATTN: DRXSY-MP ABERDEEN PROVING GROUND MARYLAND 21005	1

NOTE: PLEASE NOTIFY COMMANDER, ARRADCOM, ATTN: BENET WEAPONS LABORATORY, DRDAR-LCB-TL, WATERVLIET ARSENAL, WATERVLIET, N.Y. 12189, OF ANY REQUIRED CHANGES.

FILME

9